

## INFLUENCE OF ACTIVATION TEMPERATURE ON STRUCTURAL AND TEXTURAL PROPERTIES OF CoMo/Al<sub>2</sub>O<sub>3</sub> HYDRODESULFURIZATION CATALYST

Radoslav D. MIĆIĆ,<sup>a</sup> Radmila P. MARINKOVIĆ-NEDUČIN,<sup>b</sup> Zoltán SCHAY,<sup>c</sup> István NAGY,<sup>c</sup> Milica HADNAĐEV<sup>b</sup> and Ernő E. KISS<sup>b\*</sup>

<sup>a</sup>NIS Refinery Novi Sad, 21000 Novi Sad, Put Šajkaškog odreda 4, Serbia

<sup>b</sup>University of Novi Sad, Faculty of Technology, 21000 Novi Sad, Bulevar Cara Lazara 1, Serbia

<sup>c</sup>Institute of Isotopes, Department of Surface Chemistry and Catalysis, HAS, P.O.Box.77, H-1525 Budapest, Hungary

Received August 31, 2007

Investigations of a commercial CoMo/Al<sub>2</sub>O<sub>3</sub> hydrodesulfurization (HDS) catalyst are directed towards optimization of activation procedure of HDS catalyst concerning its active phase formation and its thermal stability. Optimization of CoMo/Al<sub>2</sub>O<sub>3</sub> catalyst properties leads to improvement of its performances varying process parameters without additional investments in equipment or catalyst replacement. Using this catalyst in conventional HDS plants, diesel with less than 50 ppm of sulfur may be achieved. The most critical step in experiments toward attainment of optimal catalytic performances is catalyst activation procedure. The object of this paper is optimization of the activation procedure by varying the activation temperature, important for formation and modification of active structure and optimal catalyst texture. Structural and textural data obtained by XRD, IR-FTIR, XPS and LTNA reveal that the optimal temperature is 300°C for the formation of active species on catalyst surface and an appropriate pore structure in catalyst bulk.

### INTRODUCTION

The main emphasis of petroleum refining during the last three decades was to maximize conversion of heavy oils to gasoline and middle distillate products. While this objective is still important, the current focus is to develop cleaner products.

Increasing concerns with environmental protection have resulted in the necessity to produce cleaner fuels, with lower impurity levels. One of the most unwanted impurities is sulfur, which is responsible for the emission of SO<sub>x</sub>. The refining industry needs to improve continuously its hydrodesulfurization (HDS) processes to satisfy the legislation, which will impose a limit of 50 ppm of sulfur in gas-oils. The understanding of the structure of the catalysts currently used is therefore of greatest interest, in order to improve their performance.<sup>1,2</sup>

Recently, there has been an increased demand for transport fuels with ultra low sulfur content, and this has resulted in many new challenges in HDS processes. In order to achieve higher sulfur

conversion, we need to remove very refractory sulfur compounds, like dialkylated dibenzothiophenes (DBT).<sup>3</sup>

Environmental regulations reduce sulfur dioxide, nitrogen oxides, aromatics, vapor emissions and particulates almost to zero-emissions.<sup>4</sup> Increase in sulfur level in the crude oil pool will also require more hydrodesulfurization capacity worldwide and improved performance of available technologies. Hydrodesulfurization is an essential process in hydrotreating and hydrocracking technologies.<sup>5,6</sup> Most important industrial HDS catalysts are the alumina supported MoO<sub>x</sub> catalysts, promoted with NiO or CoO. This extremely dynamic and flexible catalytic system during its entire life cycle, starting from the oxide form during the preparation, over the activation by sulfidation and deactivation under reaction conditions, to its return to the oxide form after regeneration undergoes substantial changes.

The activation step is crucial for the physico-chemical properties of the catalysts (nature, composition and dispersion of the active phase)

\* Corresponding author: ekiss@tehnol.ns.ac.yu

and consequently for the activity and selectivity. In particular, the temperature used in this step can deeply affect the degree of reduction and sulfidation, as well as the dispersion of the active phase.<sup>7</sup>

Results of the previous experiments show an opportunity for achievement of diesel with sulfur content less than 50 ppm by using traditional CoMo/Al<sub>2</sub>O<sub>3</sub> catalyst in the conventional HDS plant. In order to attain this aim it is necessary to increase reaction temperature and reduce space velocity as well as take care on gas recycle composition. This way of approach guarantees an optimal H<sub>2</sub>/H<sub>2</sub>S ratio toward inhibition of S-vacancies poisoning with H<sub>2</sub>S formed in desulfurization procedure.<sup>8</sup>

For the CoMo/Al<sub>2</sub>O<sub>3</sub> catalyst generally has been accepted that the active sites are the sulfided molybdenum and cobalt complex structure in interaction with the support. The well dispersed MoS<sub>2</sub> on alumina surface are edge decorated with sulfidic cobalt molecules.<sup>9</sup> The active phase is the active site plus the ensemble of transition metal and sulfur ions making this site active. The active phase is situated either on the surface of larger metal sulfide crystallites or, as very small clusters, directly on the support.<sup>10</sup> Catalyst is enabled to facilitate numerous reactions via different mechanisms owing to different MoS<sub>2</sub> dispersion grade, Co<sub>9</sub>S<sub>8</sub> segregation as well as variable S content.<sup>10, 11</sup> Large MoS<sub>2</sub> and Co<sub>9</sub>S<sub>8</sub> crystals are generally absent.<sup>10</sup> Crystalline MoO<sub>3</sub> only get sulfided on the surface while the core preserves its oxidic character or gets reduced to metal.<sup>12</sup> Completely sulfided molybdenum MoS<sub>2</sub> clusters, no longer linked to the support, can migrate over the alumina surface and sinter.<sup>13, 14</sup> As the MoS<sub>2</sub> dispersion decreases, the relative amount of cobalt on the MoS<sub>2</sub> edges gets very high.<sup>7, 15</sup> Since cobalt is not likely to be built in the MoS<sub>2</sub> matrix, segregation of Co<sub>9</sub>S<sub>8</sub> takes place.<sup>16, 17</sup>

During the oxidative regeneration large MoS<sub>2</sub> particles get oxidized exclusively on their surface and their redispersion is incomplete.<sup>10</sup> The amount of Mo<sup>4+</sup> decreased significantly, after oxidation up to 260°C, but most of sulfur remained sulfidic. Namely, predominant amount of sulfur might be attributed to oxisulfidic sulfur rather than sulfate sulfur.<sup>18</sup>

The influence of activation temperature on structural and textural properties of a commercial CoMo/Al<sub>2</sub>O<sub>3</sub> catalyst samples was performed in order to define the optimal activation temperature in laboratory conditions.

## RESULTS

### XRD and IR analysis

These bulk techniques were not sensitive enough to reveal the fine differences in highly dispersed complex active structure of the sulfided CoMo/Al<sub>2</sub>O<sub>3</sub> catalyst. To enhance the differences between the catalyst samples treated at different temperatures the samples were additionally treated at 750°C for 3 hours in nitrogen flow 30cm<sup>3</sup>/min.

The alumina support of the catalyst is in the  $\gamma$ -form [ASTM 10-425]. During the sulfidation the oxide forms of molybdenum and cobalt (MoO<sub>3</sub>, CoO) are partially converted into sulfides. Slight signals of Al<sub>2</sub>(MoO<sub>4</sub>)<sub>3</sub> [ASTM 23-764] resulted from weak interaction between active component and the catalyst support. Appearance of MoO<sub>2</sub> [ASTM 5-0452] phase can be explained by reduction of MoO<sub>3</sub> during the H<sub>2</sub>/H<sub>2</sub>S treatment of the catalyst. Molybdenum appears in two sulfided forms: MoS<sub>2</sub> [ASTM 17-744] and MoS<sub>2</sub>-H [ASTM 6-0097]. The presence of two sulfided forms of molybdenum points out that agglomeration proceeds in catalysts during its activation. Relatively strong signals from the MoS<sub>2</sub> plains at  $2\theta = 58.64^\circ$  and  $32.96^\circ$  reveal the presence of coarse sulfide particles. Presence of CoMo<sub>2</sub>S<sub>4</sub> phase is speaking about migration of molybdenum and cobalt species on the surface of catalyst support. The separation of Co<sub>9</sub>S<sub>8</sub> molecules [ASTM 19-364] from the active phase is a proof that the heat treatment at 340°C exceeds the optimal temperature of catalyst activation.

The IR-spectra of sulfided catalyst samples treated at different temperatures are very similar. Slight differences between the catalyst samples are registered in wave number range 1106-1117 cm<sup>-1</sup>. The broad absorbance signal is most expressed in sample treated at 320°C. We suppose that this broad absorbance band could be attributed to the sulfide phases. This signal is absent or very weak in the samples treated at other temperatures.

### Textural properties

The textural properties of the catalyst samples treated at different temperatures are presented in Table 1. The textural properties of the commercial CoMo/Al<sub>2</sub>O<sub>3</sub> catalyst are relatively stable in the applied experimental conditions. Sample treated at 300°C has the highest surface area, 215.5 m<sup>2</sup>/g. This value is about 20 % bigger comparing to the

lowest one (180.3 m<sup>2</sup>/g, 260°C). The average pore diameter has the lowest value in sample treated at 300°C. Considering these data the optimal temperature for catalyst texture formation could be 300°C. The subsequent heat treatment, in nitrogen atmosphere, stabilises the textural properties of CoMo/Al<sub>2</sub>O<sub>3</sub> catalyst. Nitrogen atmosphere even at

high temperature as 340°C did not cause drop of surface area of catalyst sample. The stabilizing effect of nitrogen atmosphere on textural properties of catalyst makes this inert gas very appropriate as carrier gas for oxidative regeneration of the exhausted catalyst.

Table 1

Textural properties of the sulfided CoMo/Al<sub>2</sub>O<sub>3</sub> catalyst subsequently treated in nitrogen atmosphere

Fresh Catalyst	BET Surf. area, m <sup>2</sup> /g		Pore volume, cm <sup>3</sup> /g		Average pore diameter, nm	
	H <sub>2</sub> /H <sub>2</sub> S	N <sub>2</sub>	H <sub>2</sub> /H <sub>2</sub> S	N <sub>2</sub>	H <sub>2</sub> /H <sub>2</sub> S	N <sub>2</sub>
	196.34		0.468		9.532	
Atmosphere/°C	H <sub>2</sub> /H <sub>2</sub> S	N <sub>2</sub>	H <sub>2</sub> /H <sub>2</sub> S	N <sub>2</sub>	H <sub>2</sub> /H <sub>2</sub> S	N <sub>2</sub>
240	183.9	179.8	0.442	0.464	9.61	10.32
260	180.3	193.0	0.408	0.504	9.06	10.44
280	203.5	204.1	0.472	0.540	9.28	10.58
300	215.5	198.0	0.467	0.509	8.67	10.27
320	183.2	183.1	0.443	0.499	9.68	10.91
340	187.7	195.2	0.436	0.458	9.30	9.39

### XPS analysis

The chemical state of active catalyst compounds was analysed by XPS Mo 3d and S 2s, Co 2p and S 2p transitions.

Characteristic lines of both Mo<sup>6+</sup> (232.3 and 229.2 eV,) and Mo<sup>4+</sup> (doublet of Mo<sup>4+</sup> species) appear in the spectra of all activated samples,

confirming the coexistence of both oxidation states in the active surface structure of the catalyst, as shown in Fig. 1.

The oxide and sulfide species in cobalt XP spectra are given in Fig. 2. In all XP spectra all 4 characteristic Co<sup>2+</sup> peaks are present in all the samples, Co<sup>0</sup>, CoO<sub>x</sub>, CoS and CoSO<sub>4</sub>.

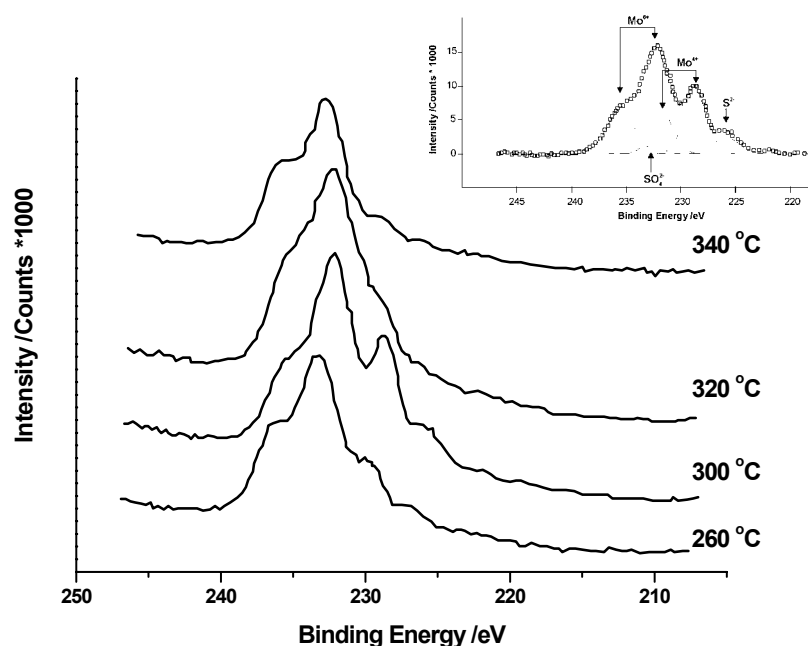


Fig. 1 – XP spectra of molybdenum in sulfided CoMo/Al<sub>2</sub>O<sub>3</sub> catalyst at different temperatures.

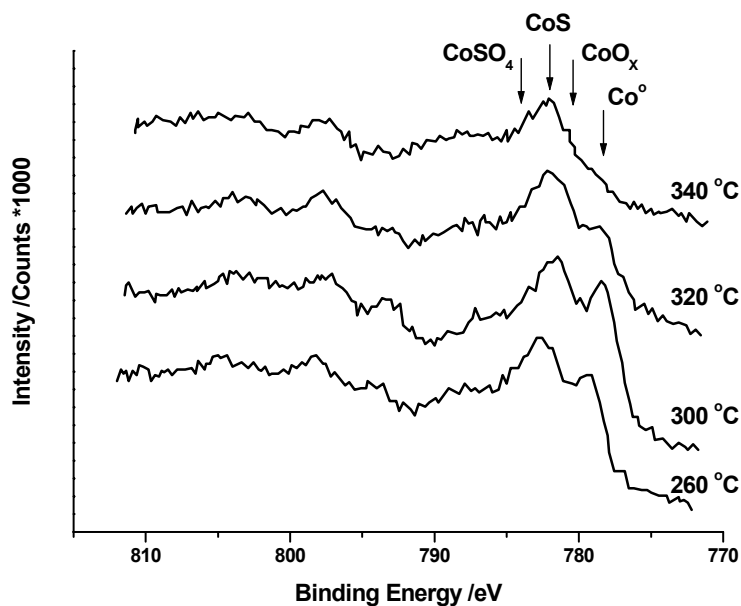


Fig. 2 – XP spectra of cobalt in sulfided CoMo/Al<sub>2</sub>O<sub>3</sub> catalyst at different temperatures.

The XP spectra of S 2p give more data about the sulfur forms present in the samples, as shown in Fig. 3. The characteristic sulfide S<sup>2-</sup> line at 161.8 ± 0.3 eV and sulfate S<sup>6+</sup> 168.8 ± 0.3 eV were

observed in the spectra. In Table 2, the quantitative interpretation of sulfide/sulfate contribution to overall sulfur content is presented.

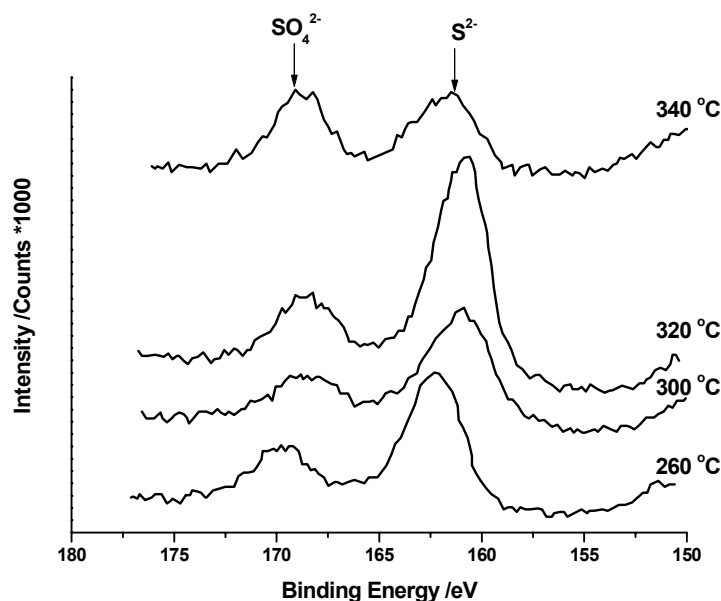


Fig. 3 – XP spectra of sulfur in sulfided CoMo/Al<sub>2</sub>O<sub>3</sub> catalyst at different temperatures.

Table 2

Quantification of the XP spectra

Temperature °C	S <sup>2-</sup> /S <sup>6+</sup> in S 2p		MoS in Mo 3d	CoS in Co 2p
	%		%	%
260	69		31	29
300	74		44	17*
320	71		35	43
340	55		24	37

\*CoS+CoSO<sub>4</sub> only 40% compared to about 70% for the other ones, balance is CoO<sub>x</sub>

## DISCUSSION

XRD and FTIR techniques were not sensitive enough to reveal the fine differences in highly dispersed complex active structure of the sulfided CoMo/Al<sub>2</sub>O<sub>3</sub> catalyst. That is the reason that the discussion of the obtained results is focused on the XPS data.

In XP spectrum of Mo 3d the 3d<sub>3/2</sub> and 3d<sub>5/2</sub> spin-doublet gives the most intensive peaks. The contribution of the S 2s transition is small due to the low sensitivity factor being about ten times smaller than that of Mo 3d. The position of the Mo 3d doublet depends on the oxidation state.<sup>19</sup> It is therefore possible to study sulfidation behaviour of molybdenum oxide catalysts by following the displacements of the doublet. For oxide forms of the catalyst the doublet of Mo<sup>6+</sup>, in similar surrounding as in MoO<sub>3</sub> and Al<sub>2</sub>(MoO<sub>4</sub>)<sub>3</sub> structures, is positioned at 235.5 eV and 232.9 eV, respectively.<sup>20</sup> The values of the binding energies of the Mo3d<sub>3/2</sub> and Mo3d<sub>5/2</sub> photoelectrons are 235.8 eV and 232.7 eV, respectively.<sup>21</sup> Generally, the binding energy of the Mo3d<sub>5/2</sub> XPS peak is ~ 233 eV, which is typical for supported Mo<sup>6+</sup> species.<sup>22</sup> In the sulfided forms, a new doublet appears which is shifted to 232.3 and 229.2 eV, respectively, due to the presence of Mo<sup>4+</sup> sulfide and/or oxide environment.<sup>18</sup> The observed broadening of the lines points out the interaction of active component with the support, as in the other catalyst of similar type.<sup>18, 23</sup> The differences in the intensities of corresponding lines give insight in the contribution of defined oxidation states of molybdenum.

The most intensive peak of Mo<sup>6+</sup> referenced to the Al 2p intensity is present in the sample treated at 340°C. We interpret this result in terms of highest content of residual oxide or sulphate forms of molybdenum at the applied activation temperature. The lowest contribution of residual oxide (sulfate) of molybdenum is observed in samples treated at 300°C and 320°C. Characteristic doublet for Mo<sup>4+</sup> species is present in all samples, shifted lower binding energies by 3.6-3.8 eV, which is consistent with literature data.<sup>24, 25</sup> The characteristic peak at 228 eV is the most intense and sharp in the sample treated at 300°C. We interpret this result in terms of most expressed sulfide surrounding of Mo<sup>4+</sup>, based on literature data on small differences in binding energies for oxide and sulfide environment of that oxidation state, 0.4-0.7 eV.<sup>26</sup> Characteristic S 2s peak at 226 eV is also present, pointing to the presence of

sulfide forms,<sup>20</sup> being also most intensive at 300°C treated sample and confirming the sulfide environment in the sample.

Similar trend concerning oxide and sulfide species is observed in cobalt XP spectra. Here the peak position at 778.3 eV is the same as that of Co<sup>0</sup>, whereas the peak at 780.4 eV is typical for CoO. The values of the binding energies of the Co2p<sub>3/2</sub> photoelectrons are between 780.1-781.9.<sup>21</sup> In all XP spectra all 4 characteristic Co<sup>2+</sup> peaks are present in all the samples, as show in Fig. 2.

The 778.3 eV peak has the highest intensity in the sample treated at 300°C, speaking also in favour of the expressed sulfiding and reduction. The Co 2p XP spectrum of the sample treated at 340°C is rather unstructured but is dominated by CoS<sub>x</sub> and CoSO<sub>4</sub> components. There is a substantial broadening of characteristic peaks in all of the samples, confirming the strong interaction of promoter species in an active structure with the support.

The XP spectra of S 2p give more data about the sulfur forms present in the samples, as shown in Fig. 3. The characteristic sulfide S<sup>2-</sup> line at 161.8 ± 0.3 eV and sulfate S<sup>6+</sup> 168.8 ± 0.3 eV were observed in the spectra,<sup>26</sup> having different intensities concerning the activation temperature applied. The authors suggest that sulfate resulted from intermediate compound state, molybdenum oxisulfide,<sup>10</sup> originated from incomplete catalyst activation and its further oxidation in ambient conditions. On the other hand, this may be the case when catalyst sample was not stored under inert conditions. The most intensive sulfide line (161.5 eV) is present after the sulfidation at 300°C, being the least one at 340°C.

The sulfate and sulfide forms are of almost identical intensities at 340 °C. The fraction of sulfide in the total sulfur depends on the temperature of the sulfidation and goes through a maximum at 300 °C treatment. The same holds for the fraction of MoS<sub>x</sub> which goes through a maximum at 300 °C sulfidation, too. The contribution of the sulfide form to the Co 2p spectra goes through a maximum at a slightly higher temperature of 320 °C, Table 2.

## EXPERIMENTAL

The activation of a typical industrial CoMo/Al<sub>2</sub>O<sub>3</sub> HDS catalyst (3.4 wt. % molybdenum and 1.2 wt. % cobalt) was studied in a fix-bed quartz U-tube flow reactor (ø = 8 mm, L = 20 cm) loaded with 4g catalyst. The catalyst density was 0.53 kg/dm<sup>3</sup>. The reactor was purged with nitrogen (30 cm<sup>3</sup>/min)

at the temperature selected for subsequent sulfidization. It was carried out in H<sub>2</sub>/H<sub>2</sub>S flow (30 cm<sup>3</sup>/min, H<sub>2</sub>/H<sub>2</sub>S = 14, GHSV 240 h<sup>-1</sup>) at 101 kPa and constant temperature in the range of 240 and 340 °C during the time sufficient to introduce ~ 4 wt.% of sulfur. The sulfided sample was cooled down to 100 °C in hydrogen flow and subsequently in nitrogen flow to room temperature.

Debye-Scherrer XRD powder analysis, (Philips APD 1700 Cu<sub>Kα</sub>) in the range 2θ = 5-70° and IR-FTIR analysis, using KBr disc technique with 0.5 wt. % of samples (Thermo Nicolet Nexus 670) in the range of 400-4000 cm<sup>-1</sup>, were applied in bulk structural investigations.

The surface composition of the sulfided catalysts was analyzed by KRATOS XSAM800 XPS machine using Al-Kα source with 120 W X-ray power and 40 eV pass energy. To avoid any artifacts the samples were used in the original form as extrudates of 1.5 mm diameter. The spectra were evaluated using the manufacturer's software. The binding energies were referenced to Al 2p at 74 eV. As the spectral region of Mo 3d is rather complicated and coincides with S 2s the procedure proposed by Paál *et al.*<sup>27</sup> was applied in the fitting. The spin separation, the intensity ratio of the spin doublet and FWHM of the different Mo states were fixed as 3.1 eV, 3:2 and 2.8 ± 0.3 eV, respectively. The ratio of the sulfur peak areas corresponding to S<sup>2-</sup> and SO<sub>4</sub><sup>2-</sup>, respectively, was taken from the S 2p spectra. The peak positions were constrained into ± 0.3 eV range as follows: S<sup>2-</sup> 226 eV, SO<sub>4</sub><sup>2-</sup> 233 eV, Mo<sup>6+</sup> 232.8 eV and Mo<sup>4+</sup> 229.2 eV. Mo<sup>5+</sup> or isolated Mo<sup>4+</sup> at 231 eV were not considered. The Co 2p<sub>3/2</sub> range was fitted with 4 peaks corresponding to Co<sup>0</sup>, CoO<sub>x</sub>, CoS<sub>x</sub> and CoSO<sub>4</sub> at binding energies: 778.3 eV, 780.4 eV, 782 eV and 784 eV, respectively. The broad LMM Auger peak appearing in the binding energy scale at 777 eV was considered in the baseline subtraction. In the fitting the peak positions were considered to ± 0.3 eV. The satellite structure between the spin-doublet as well as the Co 2p<sub>1/2</sub> was not fitted.

Textural properties were examined by low temperature N<sub>2</sub> adsorption/desorption (LTNA), Micromeritics ASAP 2000. BET adsorption isotherm and *t*-plot were applied in data processing. The pores diameter was determined by pore size distribution curve as dV/dlogD.

## CONCLUSION

The activation temperature of CoO-MoO<sub>3</sub>/γ-Al<sub>2</sub>O<sub>3</sub> catalyst affects significantly the initial active structure of HDS catalyst. XPS investigation confirmed considerable differences in the contribution of oxide/sulfide/sulfate species in activated commercial catalyst. Based on the quantification of different sulfur states and textural properties of the catalyst samples, temperature of 300 °C is estimated as optimal for activation of the selected commercial CoO-MoO<sub>3</sub>/γ-Al<sub>2</sub>O<sub>3</sub> catalyst. Nitrogen atmosphere has a stabilizing effect on the textural properties of activated catalyst.

*Acknowledgement:* The authors would like to thank the Ministry of Science and Environment Protection, Republic of

Serbia, for financial support for this paper (Project ON 142024).

## REFERENCES

1. G. Plazenet, E. Payen and J. Lynch, *Phys. Chem. Chem. Phys.*, **2002**, *4*, 3924-3929.
2. A. Griboval, P. Blanchard, L. Gengembre, E. Payen, M. Fournier, J.L. Dubois, and J.R. Bernard, *J. Catal.*, **1999**, *188*, 102-110.
3. H. Topsøe *Applied Catalysis A: General*, **2007**, *322*, 3-8.
4. M. Absi-Halabi, A. Stanislaus and H. Qabazard, *Hydrocarbon Processing* **76**, 45 (1997).
5. P. Tétényi and V. Golsán, *React. Kinet. Catal. Lett.*, **2003**, *78*, 299-308.
6. P. Tétényi and T. Koltai, *React. Kinet. Catal. Lett.*, **2004**, *82*, 371-379.
7. M. Ferrari, S. Bosmans, R. Maggi, B. Delmon and P. Grange, *Catalysis Today*, **2001**, *65*, 257-264.
8. R. Mičić, G. Bosković, *Ind. Eng. Chem. Res.*, **2006**, *45*, 7393-7398.
9. S. M. A. M. Bouwens, F. B. M. van Zon, M. P. van Dijk, A. M. van der Kraan, V. H. J. de Beer, J. A. R. van Veen and D. C. Koningsberger, *J. Catal.*, **1994**, *146*, 375-393.
10. S. Eijbouts, *Appl. Catal. A.*, **1997**, *158*, 53-92.
11. Y. Zhao and R. Prins, *J. Catal.*, **2005**, *229*, 213-226.
12. K. C. Pratt, J. V. Sanders and V. Christov, *J. Catal.*, **1990**, *124*, 416-432.
13. S. Eijbouts, J. J. L. Heinerman and H. J. W. Elzerman, *Appl. Catal. A.*, **1993**, *105*, 53-68.
14. S. Eijbouts, J. J. L. Heinerman and H. J. W. Elzerman, *Appl. Catal. A.*, **1993**, *105*, 69-82.
15. J. Cruz-Reyes, M. Avalos-Borja, M. H. Farias and S. Fuentes, *J. Catal.*, **1992**, *137*, 232-242.
16. N.-Y. Topsøe and H. Topsøe, *J. Catal.*, **1983**, *84*, 386-401.
17. J. R. Guenter, T. I. Koranyi, O. Marks and Z. Paál, *Appl. Catal.*, **1988**, *39*, 285-294.
18. Y. Yoshimura, N. Matsubayashi, H. Yokokawa, T. Sato, H. Shimada and A. Nishijima, *Ind. Eng. Chem. Res.*, **1991**, *30*, 1092-1099.
19. A. Cimino and B. A. De Angelis, *J. Catal.*, **1975**, *36*, 11-22.
20. A. Artega, J. L. G. Fierro, F. Delonnay and B. Delmon, *Appl. Catal.*, **1986**, *26*, 227-249.
21. Ch. Papadopoulou, J. Vakros, H.K. Matralis, G.A. Voyiatzis, and Ch. Kordulis, *J. Colloid and Interface Science*, **2004**, *274*, 159-166.
22. S. Dzwigaj, C. Louis, M. Breyse, M. Cattenot, V. Bellière, C. Geantet, M. Vrinat, P. Blanchard, E. Payen, S. Inoue, H. Kudo, Y. Yoshimura, *Appl. Cat. B: Environmental*, **2003**, *41*, 181-191.
23. J. S. Brinnen and W. D. Armstrong, *J. Catal.*, **1978**, *54*, 57-65.
24. T.A. Patterson, J.C. Carver, D. E. Leyden and D. M. Hercules, *J. Phys. Chem.*, **1976**, *80*, 1700-8.
25. P. Gajardo, R. I. Declerck-Grimmee, G. Delvaux, P. Olodo, J. M. Zabala, P. Canesson, P. Grange and B. Delmon, *J. Less-Common Metals*, **1977**, *54*, 311-320.
26. T. I. Koranyi, I. Manninger, Z. Paál, O. Marks and J. R. Guenter, *J. Catal.*, **1989**, *116*, 422-439.
27. Z. Paál, P. Tétényi, M. Muhler, U. Wild, J.-M. Manoli and C. Potvin, *J. Chem. Soc., Faraday Trans.*, **1998**, *94*, 459-466.